

LIQUIDUS CURVES FOR THE CRYOLITE - AlF_3 - CaF_2 - Al_2O_3 SYSTEM
IN ALUMINUM CELL ELECTROLYTES

Ray D. Peterson & Alton T. Tabereaux
Manufacturing Technology Laboratory
Reynolds Metals Company
P.O. Box 1200
Sheffield, AL 35660

Measurements of cryolitic electrolyte freezing points in the quaternary system Na_3AlF_6 - AlF_3 - CaF_2 - Al_2O_3 were conducted in order to resolve some of the apparent discrepancies reported by previous investigators. Rather than investigating just the boundaries of the quaternary system, a large number of tests were conducted in the "interior" of the defined system. This was done so that the results could be used to evaluate the freezing point of traditional bath chemistries. The freezing points of synthetic electrolyte samples were combined with accepted literature values for several of the binary boundaries to create a total data set covering the experimental range of 0 - 22% excess AlF_3 (CR = NaF/AlF_3 weight ratio = 1.50 to 0.90), 0 - 12% CaF_2 , and 0 - 5% Al_2O_3 . Five planes (one component held constant) in the experimental space were examined and fitted with isopleths for the electrolyte liquidus temperature. From the shape of the isopleths and using the complete data set, a single model for predicting freezing point temperatures was developed to cover the entire experimental range for the Na_3AlF_6 - AlF_3 - CaF_2 - Al_2O_3 electrolyte chemistry system.

INTRODUCTION

In our work of evaluating various electrolyte chemistries, we have found it useful to develop models for many of the properties associated with cryolitic electrolytes. One of these properties is the freezing point of the bath. It is necessary to know the liquidus temperature of an electrolyte so that the aluminum electrolysis cell can be operated at the proper temperature. Industrial practice has found that operating cells 10 to 15°C higher than the liquidus or freezing temperature is desirable. Temperatures lower than this value can cause operational problems such as mucking or excessive ledge building while higher temperatures lead to a loss in current efficiency due to an enhanced back reaction of aluminum oxidation.

A number of investigators have looked at portions of the cryolite - AlF_3 - CaF_2 - Al_2O_3 system. Typically, this has been an investigation of a binary system such as Na_3AlF_6 - Al_2O_3 (Foster (1), Phillips, et al. (2)); Na_3AlF_6 - AlF_3 (Foster (3), Fenerty and Hollingshead (4)); or Na_3AlF_6 - CaF_2 (Holm (5), Fenerty and Hollingshead (4)). A few investigations were of ternary systems such as

Na_3AlF_6 - AlF_3 - Al_2O_3 (Foster (6), Fenerty and Hollingshead (4)) or Na_3AlF_6 - CaF_2 - Al_2O_3 (Fenerty and Hollingshead (4)). While this work delineates the boundary conditions of this four-component system, it does not provide details on the interactions occurring when all four components are present as in classical cryolitic baths used in aluminum electrolysis. The research group of Lee, Lei, Xu, and Brown (7) examined selected points within the Na_3AlF_6 - AlF_3 - CaF_2 - Al_2O_3 system. The results of all of the previously mentioned studies have been presented as phase diagrams. Phase diagrams do not lend themselves easily to model development applications although equations can be derived which express these relationships.

A few authors have presented multicomponent models for liquidus temperatures of electrolytes, but most of the models have certain limitations. Dewing (8) presented a regression analysis model based primarily on literature data and the assumption that small amounts of most additives (except NaF and AlF_3) will lower the liquidus temperature linearly. This model does not account for any interactions that might occur. Young and Loutfy (9) presented a linear model for liquidus temperature for the Na_3AlF_6 - AlF_3 - CaF_2 - Al_2O_3 - LiF system. Their regression model was based on a limited number of data points and was linear in cryolite ratio, a fact not observed experimentally. Bullard and Przybycien (10) presented a liquidus temperature model similar to Dewing's model. Literature values were used to modify and extend Dewing's equation. The new model was compared against 36 measured compositions. The model included first order terms for Al_2O_3 , CaF_2 , LiF , and MgF_2 , and higher order terms for excess AlF_3 and Al_2O_3 . Tabereaux (11) presented a model with probably the most extensive coverage of a wide range of electrolyte compositions to date. However, in an effort to linearize the data over the wide variation in cryolite ratio or excess aluminum fluoride, he was forced to develop four separate equations to cover the range. This makes use of the model somewhat cumbersome. Also, upon subsequent review it was observed that some of the experimental data was ill-posed causing the regression equations to be less sensitive to independent changes of single components.

The goal of this study was to develop a single model to cover the entire experimental region common to classical bath chemistry, $\text{Na}_3\text{AlF}_6 - \text{AlF}_3 - \text{CaF}_2 - \text{Al}_2\text{O}_3$. For this study, this region was defined as 0 - 22% excess aluminum fluoride (NaF/AlF_3 weight ratio = 1.5 to 0.90), 0 - 12% calcium fluoride, and 0 - 5% alumina. Alumina values were kept to 5% or less to avoid solubility problems at higher excess aluminum fluoride concentrations. This region of experimentation is presented visually in Figure 1 as a three dimensional space. At the origin is a pure cryolite, Na_3AlF_6 . Excess aluminum fluoride is denoted by the distance out from the origin on the x-axis. Similarly, the calcium fluoride is assigned to the y-axis, and the alumina is assigned to the z-axis. A binary phase diagram would be characterized as a single line in this space, while a ternary phase diagram would represent a plane on the figure. However, operational cryolitic electrolytes would be found in the "interior" of this space where little or no work has been done.

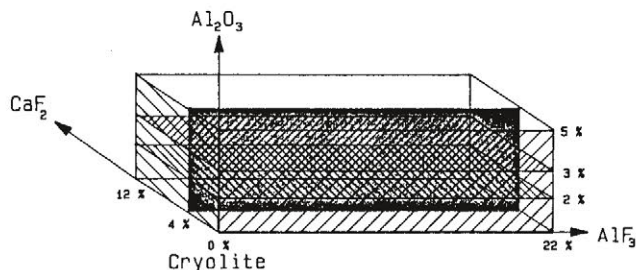


Figure 1 - Experimental space of the $\text{Na}_3\text{AlF}_6 - \text{AlF}_3 - \text{CaF}_2 - \text{Al}_2\text{O}_3$ system as studied in this paper and the five experimental planes.

To develop a model, data is needed. We used two sources for our model data:

1. Liquidus temperatures of electrolytes in the interior experimental space were determined experimentally. The experimental procedure will be discussed below.
2. Phase diagrams from literature sources were carefully examined, and checked against our experimental results for consistency. The data of Foster (6) for the $\text{Na}_3\text{AlF}_6 - \text{AlF}_3 - \text{Al}_2\text{O}_3$ system was used up to the 20% excess AlF_3 and 5% Al_2O_3 point to define the $\text{Na}_3\text{AlF}_6 - \text{AlF}_3 - \text{Al}_2\text{O}_3$ plane of the experimental space.

EXPERIMENTAL PROCEDURE

The compositions for which liquidus temperature measurements were measured were carefully planned in advance to derive the maximum sensitivity for the coefficients of each component and to allow easy examination of the results in order to derive an equation of the proper form. In addition to the $\text{Na}_3\text{AlF}_6 - \text{AlF}_3 - \text{Al}_2\text{O}_3$ plane, four other planes were investigated: $\text{Na}_3\text{AlF}_6 - \text{CaF}_2 - \text{Al}_2\text{O}_3$, $\text{Na}_3\text{AlF}_6 - \text{AlF}_3 - \text{Al}_2\text{O}_3 - 4\% \text{CaF}_2$, $\text{Na}_3\text{AlF}_6 - \text{AlF}_3 - \text{CaF}_2 - 2\% \text{Al}_2\text{O}_3$, and $\text{Na}_3\text{AlF}_6 - \text{AlF}_3 - \text{CaF}_2 - 3\% \text{Al}_2\text{O}_3$. These planes are shown in Figure 1. Each of these planes was defined by a number of tests conducted on synthetic electrolyte

samples. Chemicals from Cerac Incorporated (Milwaukee, Wisconsin) claiming +99% purity were used. However, all materials were analyzed for exact composition first. A computer program was used to solve five simultaneous equations based on mass balances to determine the exact weight of each component to add to get the desired electrolyte composition. A number of the samples were later checked by chemical analysis and found to be within the experimental limits of the analytical techniques used to define the composition.

The differential thermal analysis (DTA) technique used to determine liquidus temperatures from cooling curves has already been discussed (11) so only the major details will be given here. A schematic of the heating section of the DTA apparatus is shown in Figure 2. A twin container graphite crucible was used for measuring freezing points of the electrolytes. A 20 gram sample of the synthetic electrolyte was mixed and then melted in a graphite crucible by a 17 kVA Lepel induction furnace. A major portion of the molten electrolyte was then poured into the sample chamber of the twin chambered graphite crucible. The entire crucible arrangement was heated in the induction furnace to approximately 50°C over the electrolyte melting temperature. At this point, the power was switched off and the thermocouples were inserted into the sample and the alumina reference. As the assembly cooled, the two thermocouples maintained the same temperature until the electrolyte began to freeze and experienced a thermal arrest. This point was very easily identified on the X-Y plot generated by the thermocouples. The liquidus temperature was read from a digital thermometer as the arrest occurred. Reproducibility of liquidus temperature was $\pm 1^\circ\text{C}$ between separately mixed samples of the same composition. Before testing each group of samples, the DTA system was checked by determining freezing points of reagent grade LiF and NaF . If these measured values were not accurate to $\pm 1^\circ\text{C}$, the system was checked for mechanical and electrical faults and then corrected.

RESULTS AND DISCUSSION

A total of 89 experiments were performed in the "interior" of the experimental space. Also, 35 data points from Foster's work (6) were used to define the $\text{Na}_3\text{AlF}_6 - \text{AlF}_3 - \text{Al}_2\text{O}_3$ plane. The entire space was defined by a total of 124 points specified by composition and liquidus temperatures. As previously mentioned, the data was laid out by planes as shown in Figure 1. Figure 3 shows the data for the plane $\text{Na}_3\text{AlF}_6 - \text{AlF}_3 - \text{CaF}_2 - 3\% \text{Al}_2\text{O}_3$. In this figure, the origin is 97% Na_3AlF_6 and 3% Al_2O_3 . The x-axis is still the aluminum fluoride concentration while the other axis is the calcium fluoride concentration. Each square represents one synthetic electrolyte sample with 3% alumina and the corresponding amounts of AlF_3 and CaF_2 . Printed alongside of each electrolyte sample is the corresponding liquidus temperature.

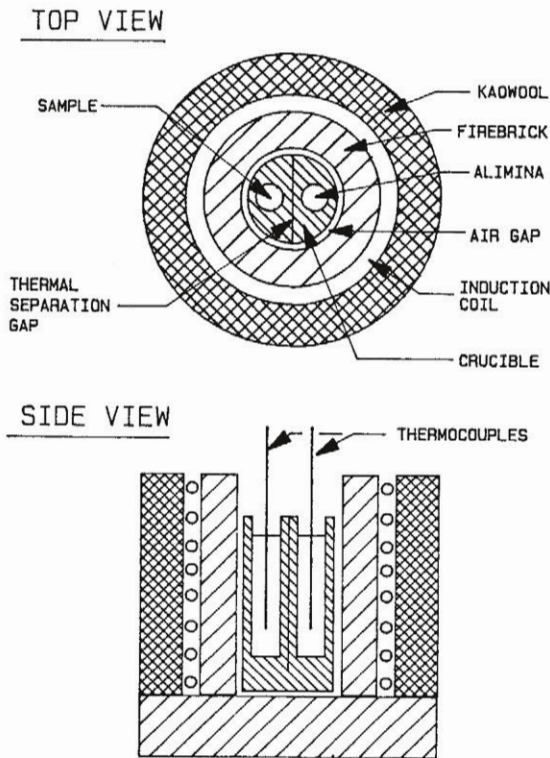


Figure 2 • Furnace and crucible design for the differential thermal analysis equipment.

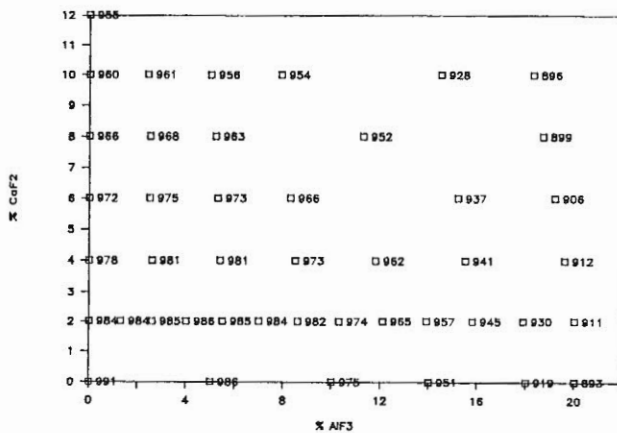


Figure 3 • Experimental data for the $\text{Na}_3\text{AlF}_6 - \text{AlF}_3 - \text{CaF}_2 - 3\% \text{Al}_2\text{O}_3$ plane.

A contouring computer program was used to draw in isopleths of the liquidus temperatures. This program uses a Kriging technique (12) which takes into account all data points within a specified radius to draw smooth lines through the grid system. All data points within the radius are weighed by their distance from the calculated grid point in the Kriging calculation, consequently an erroneous data point will skew a nearby isopleth, but have a very minor effect on distant ones. The data of the previous figure and the calculated isopleths for liquidus temperatures

are shown in Figure 4. Customarily, a ternary plot such as this would be presented in an equilateral triangle layout, but for this portion of the presentation, we will keep the rectilinear layout to avoid confusion with the earlier format. Using this contouring technique enhances the researchers' ability to observe the relationships occurring between various independent variables and the measured liquidus values. For example, in Figure 4 it can be seen that liquidus temperature is not a linear function of the CaF_2 content and the excess AlF_3 content. It appears that a cross product term probably exists. This sort of contouring was done for each of the experimental planes to help visualize the relationships occurring.

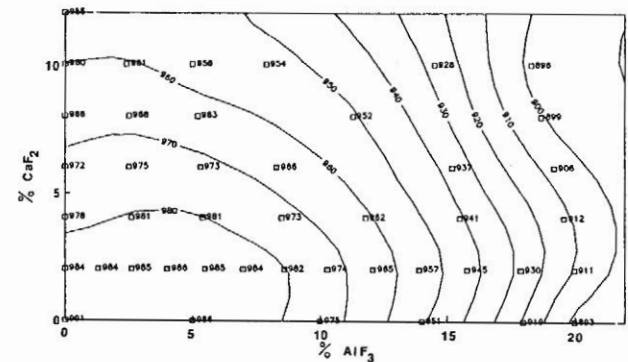


Figure 4 • Experimental data for the $\text{Na}_3\text{AlF}_6 - \text{AlF}_3 - \text{CaF}_2 - 3\% \text{Al}_2\text{O}_3$ plane and the liquidus isopleths based on the Kriging technique.

In reviewing the data used in the previous paper (11), the freezing point determination tests were run at constant additions, but with increasing excess AlF_3 . It was observed that most of the curves generated in this manner had a very strong relationship to the fundamental $\text{Na}_3\text{AlF}_6 - \text{AlF}_3$ curve. In general, the curves were displaced to a lower temperature at 0% excess aluminum fluoride (CR=1.5), but if the curves were extrapolated in the excess AlF_3 direction, they seemed to intersect at approximately the same location. Based on this observation, we felt that if the fundamental $\text{Na}_3\text{AlF}_6 - \text{AlF}_3$ curve could be accurately described, then the deviations from this line due to the various additions could be more easily characterized.

According to Foster, the liquidus temperature curve for the $\text{Na}_3\text{AlF}_6 - \text{AlF}_3$ system begins at 1009°C for pure cryolite (0% excess aluminum fluoride) and then decreases 269°C to 740°C at the peritectic. This curved line can be approximated by a cosine function of the form:

$$T = 740 + 269\cos [A(\% \text{AlF}_3)]^n \quad (1)$$

where A and n are equation constants. At 0% excess AlF_3 , the function would equal 1009°C. Using Foster's data, the constants were determined by a regression equation to be $A = 3.262$ and $n = 0.4871$. The fundamental curve was defined as:

$$T = 740 + 269 \cos [3.262(\% \text{AlF}_3)]^{0.4871} \quad (2)$$

The second step in constructing a liquidus temperature model was to develop an equation for the deviation of liquidus temperatures for samples with added constituents from that of the fundamental curve. The deviation was defined as:

$$\Delta T_{\text{Dev}} (\% \text{AlF}_3, \% \text{Al}_2\text{O}_3, \% \text{CaF}_2) =$$

$$T_{\text{Exp}} (\% \text{AlF}_3, \% \text{Al}_2\text{O}_3, \% \text{CaF}_2) - T_{\text{Fund}} (\% \text{AlF}_3) \quad (3)$$

A multiple linear regression was performed on the data set containing the 124 experimental points. As a first attempt, only a linear combination of CaF_2 and Al_2O_3 was used. The regression was on the equation:

$$\Delta T_{\text{Dev}} = b_1(\% \text{CaF}_2) + b_2(\% \text{Al}_2\text{O}_3) \quad (4)$$

This linear combination proved unsatisfactory, so various combinations of cross products composed of each of the additives were tried. The best combination of terms, both linear and cross products was determined to be:

$$\begin{aligned} \Delta T_{\text{Dev}} = & - 5.0271(\% \text{Al}_2\text{O}_3) - 2.7056(\% \text{CaF}_2) \\ & - 0.3717(\% \text{Al}_2\text{O}_3)^{1/2}(\% \text{CaF}_2) \\ & - 0.00646(\% \text{Al}_2\text{O}_3)^{1/2}(\% \text{AlF}_3)^2 \\ & + 0.9580(\% \text{CaF}_2)^{1/2}(\% \text{AlF}_3) \\ & - 0.1199(\% \text{CaF}_2)(\% \text{Al}_2\text{O}_3)^{1/2}(\% \text{AlF}_3) \quad (5) \end{aligned}$$

All of these terms were determined to be statistically significant. The multiple correlation coefficient (r^2) was calculated to be 0.9720 or 97.2% of the deviation from the fundamental curve due to various components could be accounted for by this regression equation.

Equation (5) is combined with Equation (2) to yield the final equation for liquidus temperature. The equation is:

$$\begin{aligned} T = & 740 - 5.0271(\% \text{Al}_2\text{O}_3) - 2.7056(\% \text{CaF}_2) \\ & - 0.3717(\% \text{Al}_2\text{O}_3)^{1/2}(\% \text{CaF}_2) \\ & - 0.00646(\% \text{Al}_2\text{O}_3)^{1/2}(\% \text{AlF}_3)^2 \\ & + 0.9580(\% \text{CaF}_2)^{1/2}(\% \text{AlF}_3) \\ & - 0.1199(\% \text{CaF}_2)(\% \text{Al}_2\text{O}_3)^{1/2}(\% \text{AlF}_3) \\ & + 269 \cos [3.262(\% \text{AlF}_3)]^{0.4871} \quad (6) \end{aligned}$$

The mean sum of square of the error between experimental values and model values is 2.56°C . This is not much higher than the experimental error of the measuring system.

The cross product terms were added to handle the interactions between compounds added to the electrolyte. For instance, in Figure 3 with the raw experimental data for liquidus temperature and in Figure 4 with liquidus temperature isopleths, it can be observed that the addition of CaF_2 changes the shape of the fundamental $\text{Na}_3\text{AlF}_6 - \text{AlF}_3$ curve. At 2% CaF_2 , the liquidus temperature starts at 984°C at 0% excess AlF_3 , rises to 986°C at 4.3%, and then drops down again. A cross product term would obviously be needed in this case. Each of the cross product terms was added only when it would significantly improve the fit of the model to the data.

The linear terms for CaF_2 and Al_2O_3 are in general agreement with other investigators. At low concentrations of these components and at the cryolite composition, only the linear terms will be significant. For CaF_2 , our linear term has a value of $-2.706^\circ\text{C}/\%$ added while Bullard and Przybycien found -2.962 , and Dewing found -2.853 . The Lee, Lei, Xu, and Brown liquidus equation (7) found a linear term of $+4.059^\circ\text{C}/\%$ and had a second order term of $-1.167^\circ\text{C}/(\% \text{ added})^2$. Undoubtedly, this positive term was introduced into the regression due to the range over which the regression was done. Another factor contributing to this coefficient's value may be that no uncoupled data was used in the regression. Lee, Lei, Xu, and Browns' equation is valid only in the range 3.8 to 11.2 % CaF_2 . A similar comparison for Al_2O_3 finds our linear term equaling $-5.027^\circ\text{C}/\%$ added while Bullard and Przybycien found -5.471 , Dewing found -6.646 , and Lee, Lei, Xu, and Brown found -5.33 . Dewing included a second order alumina term while the others did not.

Liquidus isopleths based on the model (Equation (6)) are shown in Figure 5 along with the experimental data for the same plane previously shown. The shape of the curves is very similar to those based directly on the data and the Kriging technique. The model produces curves which are smoother. In general, the contours seem to correspond with the data points well.

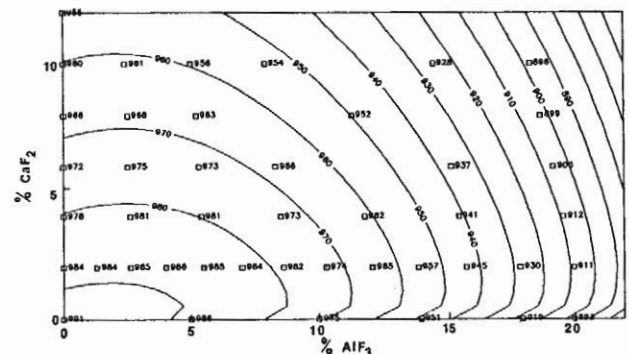


Figure 5 - Experimental data for $\text{Na}_3\text{AlF}_6 - \text{AlF}_3 - \text{CaF}_2 - 3\% \text{Al}_2\text{O}_3$ plane and the liquidus isopleths based on the regression model.

Like Bullard and Przybycien, we found that neither our experimental data nor our model agreed with Lee, Lei, Xu, and Brown's work. We did find that the general shape of the liquidus isopleths agreed with the shape proposed by Lee, Lei, Xu, and Brown though not with as an extreme hump in the liquidus line as they had determined. In the current study, at low excess AlF_3 and moderate amounts of CaF_2 , the change in liquidus temperature is very small and only slightly humped as aluminum fluoride content is increased.

Bullard and Przybycien base their liquidus temperature on the last peak seen in a heating curve from a DTA measurement since they were unable to reproducibly measure the liquidus temperature in the cooling mode due to supercooling of the sample. They also noted that changing the heating rate caused the second peak to shift slightly. They synthesized three electrolyte samples and compared their liquidus temperature results with those of Fenerty and Hollingshead (4), and Foster (6). They found agreement of liquidus temperatures within several degrees. Using our model on the same electrolyte compositions gives agreement to literature values within 0.5 degrees. All these synthesized samples contained less than 5% AlF_3 . In comparing our model with Bullard and Przybycien's experimental results, the agreement is good to approximately 6% AlF_3 . From that point on, their liquidus temperatures all become consistently low whether compared with our model or with similar experimental data. It may be in this region of higher excess aluminum fluoride that using a heating curve to determine the liquidus temperature of a complex polyphase electrolyte may not be appropriate and this might account for the discrepancy. The three models and their experimental ranges are shown in Figure 6 along with a set of liquidus curves for each model.

A comparison of measured and calculated liquidus temperatures for industrial electrolytes is presented in Table I. Since the baths contain small amounts of lithium fluoride and magnesium fluoride, and the derived model does not include their effects, an assumption of linear behavior with respect to their effect on depressing the liquidus temperature has been assumed. The linear values reported by Bullard and Przybycien (10) were used. They are $-4.6^\circ C/\%$ MgF_2 added and $-9.2^\circ C/\%$ LiF added. The measured liquidus temperatures are slightly lower than calculated values in all cases. The systematic error may be due to the use of Bullard and Przybycien's terms or may be related to a small error in the synthesis of the original electrolyte samples from which the model was derived.

CONCLUSIONS

Research work has extended the study of liquidus temperatures from the binary and ternary boundaries into the interior of the cryolite - AlF_3 - CaF_2 - Al_2O_3 system. Classical bath chemistries can now be evaluated in terms of liquidus temperature by a single mathematical expressions as given by Equation (6).

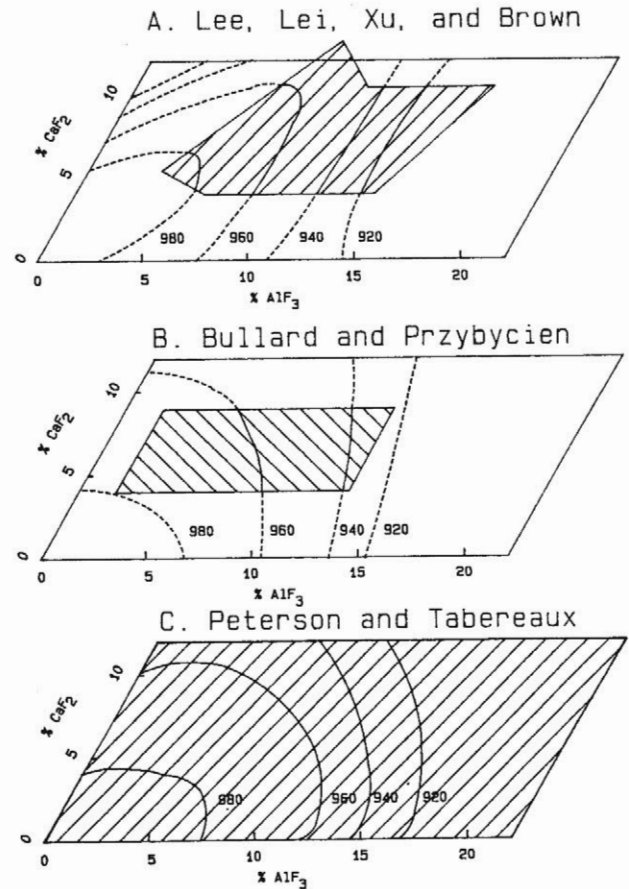


Figure 6 • Comparison of liquidus isopleths based on three different models in the 97% Na_3AlF_6 - 3 Al_2O_3 plane. The experimental range from which each model was derived is shown in cross hatching.

Table I. Comparison of Measured and Calculated Liquidus Temperatures for Industrial Electrolytes

% AlF_3	% Al_2O_3	% CaF_2	% LiF	% MgF_2	Electrolyte Liquidus Temperatures	
					Measured	Calculated
2.7	4.8	7.9	0.4	0.6	947	950.3
3.2	2.9	7.9	0.4	0.6	955	962.4
3.0	4.2	7.7	0.4	0.5	952	955.2
3.5	4.7	7.3	0.4	0.5	949	953.1
4.7	6.9	3.3	1.6	2.5	931	932.7
5.5	3.7	3.2	1.6	2.6	947	949.8
6.2	5.5	3.2	1.5	2.6	936	938.9
6.7	6.8	3.1	1.3	2.2	931	934.5

ACKNOWLEDGEMENTS

The authors would like to acknowledge the assistance of two of their colleagues. First, Mr. John O. Cook for performing the many experiments with great diligence, and secondly, Dr. Roderick Craig for his discussions on possible types of equations to fit the liquidus data.

REFERENCES

1. P. A. Foster, Jr., "Determination of the Cryolite - Alumina Phase Diagram by Quenching Methods," Journal of the American Ceramic Society, Vol. 43, 1960, pp. 66-68.
2. N. W. F. Phillips, R. H., Singleton, and E. A. Hollingshead, "Liquidus Curves for Aluminum Cell Electrolyte I," Journal of the Electrochemical Society, Vol. 102, 1955, pp. 648-649.
3. P. A. Foster, Jr., "Phase Equilibria in the System $\text{Na}_3\text{AlF}_6 - \text{CaF}_2$," Journal of the American Ceramic Society, Vol. 53, 1970, pp. 598-600.
4. A. Fennerty and E. A. Hollingshead, "Liquidus Curves for Aluminum Cell Electrolyte III," Journal of the Electrochemical Society, Vol. 107, 1960, pp. 993-997.
5. J. L. Holm, "The Phase Diagram of the System $\text{Na}_3\text{AlF}_6 - \text{CaF}_2$," Acta Chemica Scandinavica, Vol. 22, 1968, pp. 1004-1010.
6. P. A. Foster, Jr., "Phase Diagram of a Portion of the System $\text{Na}_3\text{AlF}_6 - \text{AlF}_3 - \text{Al}_2\text{O}_3$," Journal of the American Ceramic Society, Vol. 58, 1975, pp. 288-291.
7. S. S. Lee, K. Lei, P. Xu, and J. J. Brown, "Determination of Melting Temperatures and Al_2O_3 Solubilities for Hall Cell Electrolyte Compositions," Light Metals 1984, pp. 841-855.
8. E. W. Dewing, "Liquidus Curves for Aluminum Cell Electrolyte V," Journal of the Electrochemical Society, Vol. 117, 1970 pp. 770-781.
9. S. Young and R. O. Loutfy, "The Influence of LiF and Bath Ratio on Properties of Hall Cell Electrolytes," Physical Chemistry of Extractive Metallurgy, V. Kudryk and Y. K. Rao, eds., The Metallurgical Society, Warrendale, PA, 1985, pp. 263-273.
10. G. L. Bullard and D. O. Przybycien, "DTA Determinations of Bath Liquidus Temperatures: Effect of LiF," Light Metals 1986, pp. 437-444.
11. A. T. Tabereaux, "Phase and Chemical Relationships of Electrolytes for Aluminum Reduction Cells," Light Metals 1985, pp. 751-761.
12. B. D. Ripley, Spatial Statistics, Wiley-Interscience, 1981, p. 352.